



Rapid development of stable transgene CHO cell lines by CRISPR/Cas9-mediated site-specific integration into C12orf35

Menglin Zhao¹ · Jiaxian Wang^{1,2} · Manyu Luo¹ · Han Luo¹ · Meiqi Zhao¹ · Lei Han¹ · Mengxiao Zhang¹ · Hui Yang¹ · Yueqing Xie³ · Hua Jiang³ · Lei Feng⁴ · Huili Lu¹ · Jianwei Zhu^{1,3}

Received: 26 December 2017 / Revised: 12 April 2018 / Accepted: 13 April 2018 / Published online: 22 May 2018
© Springer-Verlag GmbH Germany, part of Springer Nature 2018

Abstract

Chinese hamster ovary (CHO) cells are the most widely used mammalian hosts for recombinant protein production. However, by conventional random integration strategy, development of a high-expressing and stable recombinant CHO cell line has always been a difficult task due to the heterogenic insertion and its caused requirement of multiple rounds of selection. Site-specific integration of transgenes into CHO hot spots is an ideal strategy to overcome these challenges since it can generate isogenic cell lines with consistent productivity and stability. In this study, we investigated three sites with potential high transcriptional activities: C12orf35, HPRT, and GRIK1, to determine the possible transcriptional hot spots in CHO cells, and further construct a reliable site-specific integration strategy to develop recombinant cell lines efficiently. Genes encoding representative proteins mCherry and anti-PD1 monoclonal antibody were targeted into these three loci respectively through CRISPR/Cas9 technology. Stable cell lines were generated successfully after a single round of selection. In comparison with a random integration control, all the targeted integration cell lines showed higher productivity, among which C12orf35 locus was the most advantageous in both productivity and cell line stability. Binding affinity and N-glycan analysis of the antibody revealed that all batches of product were of similar quality independent on integrated sites. Deep sequencing demonstrated that there was low level of off-target mutations caused by CRISPR/Cas9, but none of them contributed to the development process of transgene cell lines. Our results demonstrated the feasibility of C12orf35 as the target site for exogenous gene integration, and strongly suggested that C12orf35 targeted integration mediated by CRISPR/Cas9 is a reliable strategy for the rapid development of recombinant CHO cell lines.

Keywords CHO · Site-specific integration · CRISPR/Cas9 · Cell line development · C12orf35

Electronic supplementary material The online version of this article (<https://doi.org/10.1007/s00253-018-9021-6>) contains supplementary material, which is available to authorized users.

✉ Huili Lu
roadeer@sjtu.edu.cn

✉ Jianwei Zhu
jianweiz@sjtu.edu.cn

¹ Engineering Research Center of Cell and Therapeutic Antibody, Ministry of Education, School of Pharmacy, Shanghai Jiao Tong University, 800 Dongchuan Road, Shanghai 200240, China

² Present address: Department of Hematology, VU University Medical Center, Amsterdam, the Netherlands

³ Jecho Laboratories, Inc., 7320 Executive Way, Frederick, MD 21704, USA

⁴ Instrumental Analysis Center, Shanghai Jiao Tong University, Shanghai 200240, China

Introduction

Mammalian cells are the dominant hosts for production of recombinant therapeutic proteins, especially for proteins requiring complex post-translational modifications. Chinese hamster ovary (CHO) is the most commonly used mammalian cell line for the industrial production of recombinant proteins due to its significant advantages, including the human-like post-translational modifications, industrial scalability, and so on (Fischer et al. 2015; Galleguillos et al. 2017; Zhu 2012). The traditional method to obtain high-expressing recombinant CHO (rCHO) cell lines for industrial production is random integration of the recombinant protein gene (r-protein gene). To obtain a clone with high expressing level, multiple rounds of screening by a selective marker is obligatory (Lai et al. 2013; Zhu 2013). Moreover, due to lack of control of insertion sites in random integration, protein productivity of some selected clones may diminish over time, causing instability of

cell lines. Site-specific integration is thus a promising strategy to improve the development efficiency.

Several approaches have been employed to achieve site-specific integration. The first kind is mediated by site-specific recombinases including Flp/FRT (Baser et al. 2016), Bxb1 (Inniss et al. 2017), Cre/loxP, and phiC31/R4 integrases (Damavandi et al. 2017; Kawabe et al. 2016). Typically, this kind of system requires the establishment of cell line platforms for target gene integration. The second kind of system is mediated by engineered nucleases such as transcription activator-like effector nucleases (TALENs) (Sakuma et al. 2015), zinc-finger nucleases (ZFNs) (Gupta and Shukla 2017; Jabalameli et al. 2015), and clustered regularly interspaced short palindromic repeats (CRISPR)-associated (Cas) RNA guided nucleases (Bachu et al. 2015; He et al. 2016; Lee et al. 2016; Lee et al. 2015). These nucleases can induce a DNA double-strand break (DSB) at a desired site of the genome, triggering the homology-directed repair (HDR) insertion of the exogenous transgene into the DSB location. In comparison with TALENs and ZFNs, CRISPR/Cas9 technology is more efficient, reliable, and cost-effective. Using a single guide RNA (sgRNA) fused by the CRISPR RNAs (crRNAs) with a trans-activating crRNA (tracrRNA), the Cas9 protein can be directed to cleave target DNA and induce the DSB at the specified loci, to generate site-specific integration by HDR in the presence of plasmid-harboring homology arms (Cong et al. 2013). CRISPR/Cas9 has already been successfully applied for the insertion of targeted genes in many types of cell lines for fundamental research, including CHO cells (Irion et al. 2014; Lee et al. 2016; Nakao et al. 2016). However, the use of this strategy for industrial purposes remained to be investigated.

In this study, we attempted to construct a CRISPR/Cas9-mediated site-specific integration strategy to improve development process of rCHO cell lines. Due to the lack of systematic research regarding desired integration sites with high expression and stability, we selected three possible candidate sites based on previous reports. The first was a telomeric region of chromosome 8 referred to as C12orf35. It was reported that the transgenes located near the telomeric region were more stable and productive than other types of clones (Li et al. 2016; Ritter et al. 2016). The second site was HPRT, which has been reported to be an ideal integration site capable of generating high-expressing stable CHO cell lines for scFv-Fc expression (Kawabe et al. 2017; Wang et al. 2017). The third was GRIK1, a de novo integration site that has been recently discovered by identification and re-targeting efforts for transcriptional hot spots in the human genome (Cheng et al. 2016). Genes encoding mCherry and anti-PD1 monoclonal antibody (mAb) were used as model proteins to insert into above selected sites for further evaluations. Finally, we identified C12orf35 to be the optimal integrating site to obtain stable cell lines with consistent productivity and product

quality, and demonstrated that CRISPR/Cas9-mediated site-specific integration at C12orf35 is a reliable and efficient strategy to develop rCHO cell lines for industrial purposes.

Materials and methods

Cells and culture media

The adherent CHO-K1 (Invitrogen, Carlsbad, CA, USA) cells were maintained in high glucose DMEM supplemented with 10% FBS and incubated at 37 °C with 5% CO₂ in a humidified cell incubator (Thermo Fisher Scientific, Waltham, MA, USA) (Sun et al. 2015). The suspension CHO-S (Invitrogen, Carlsbad, CA, USA) cells were cultured with CD CHO medium supplemented with 8 mM L-GlutaMax in 125-mL shake flasks (Corning, Corning, NY, USA) at 37 °C with 125 rpm and 8% CO₂ (Zong et al. 2017). All media and supplements were purchased from Gibco (Thermo Fisher Scientific, Waltham, MA, USA). Cell growth and viability were monitored with a cell counter (Countstar, Shanghai, China).

Expression vector design and construction

Vectors carrying sgRNAs and GFP-Cas were designed for each potential locus as presented in Figs. 1 and 2. The single strand oligo sgRNAs were synthesized, phosphorylated, annealed, and ligated to a pX458 plasmid. Donor plasmids harboring site-specific 5' and 3' homology arms (750 bp for each), protein expression cassette (hCMV-promoter, protein-encoding genes, BGH pA), puromycin expression cassette (PGK-promoter, puromycin, BGH pA), and pUC19 backbone (Takara, Tokyo, Japan), were constructed using ClonExpress MultiS One Step Cloning Kit (Vazyme, Shanghai, China), according to manufacturer's instructions (Figs. 1a and 2a, b). We also added two CRISPR target sequences (sgRNA+ PAM) of 23 bp length which flanked the insertion fragment for both mCherry and anti-PD1 donor plasmids, which can facilitate the linearization of the fragment by Crispr/Cas9 after entering the nucleus (Fig. 2a). All primers used were synthesized by Invitrogen (Shanghai, China) and are listed in Supplementary Table S1. All components of the plasmid were amplified using PrimeSTAR Max (Takara, Tokyo, Japan) by PCR, under the following settings: 95 °C for 10 s, 55 °C for 5 s, 72 °C for 10 s, 35 cycles. All plasmids were purified using Plasmid DNA mini Kit (OMEGA Bio-Tek, Guangzhou, China) and sequenced at Invitrogen.

Plasmid transfection and sgRNAs screening for high indel efficiency

CHO-K1 cells were transfected with Lipofectamine 2000 reagent (Invitrogen, Carlsbad, CA, USA), and CHO-S cells

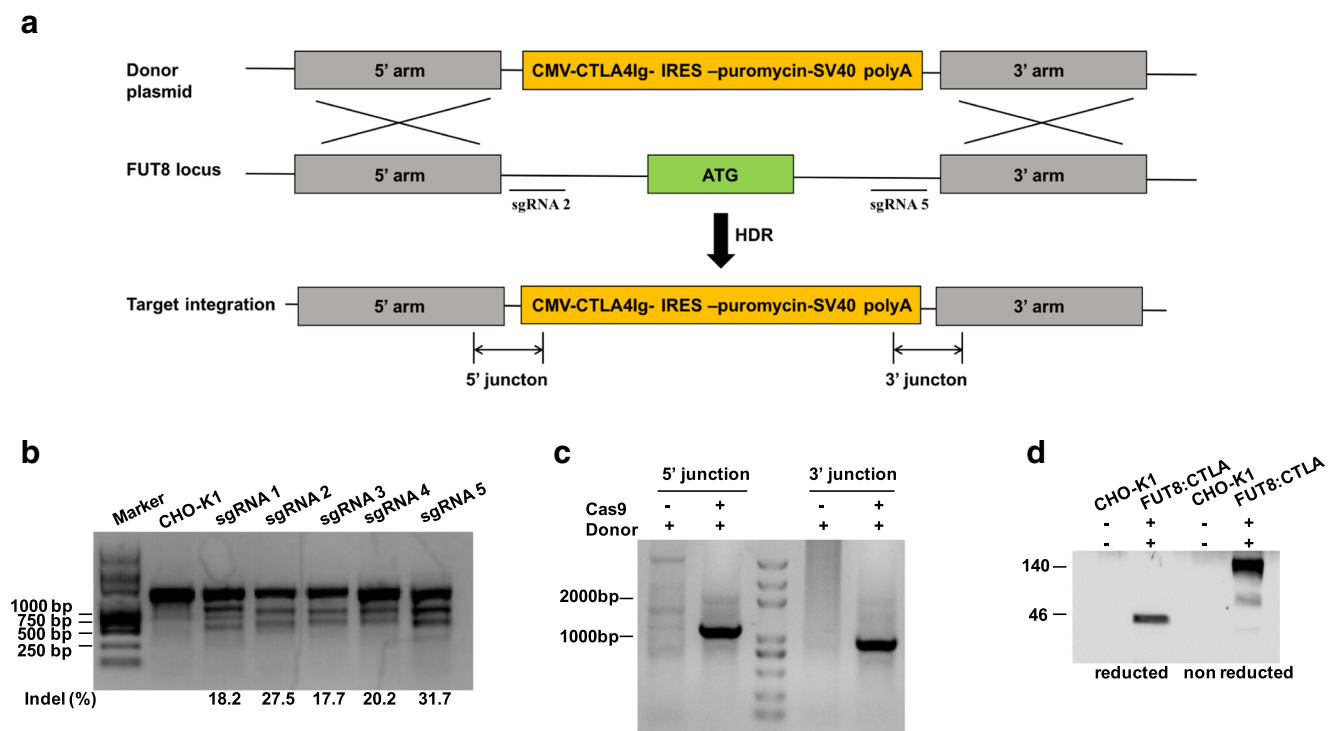


Fig. 1 Schematic illustration of FUT8 gene targeted integration in CHO-K1 cell lines. **a** HDR-based targeted integration strategy at FUT8 loci. **b** The editing efficiency of five sgRNAs targeting the FUT8 gene was estimated by the photodensity scanning of electrophoresed PCR fragments digested by T7EI. The size of un-digested PCR products for wild type was about 1500 bp; for CRISPR-Cas9 edited cells, small fragments were produced by T7EI digestion. **c** The agarose gel results of 5'/3'

junction PCR. The expected fragment sizes were all about 1200 bp. **d** Western blot of integrated cell clone or wild-type CHO-K1 cells for expression of CTLA4Ig. The bands indicated the correct insertion of CTLA4Ig, but the positions of both non-reducing and reduced samples were higher than predicted (46 kDa for CTLA4Ig monomer), possibly due to the glycosylation

were transfected by Neon Transfection System Starter Pack (Thermo Fisher Scientific; Waltham, MA, USA) with sgRNA carrying plasmids according to the manufacturer's instructions. Three days after transfection, the genome DNA was extracted using the Genomic DNA Extraction Kit (Axygen, San Francisco, CA, USA) and amplified with specific sequence primers (Supplementary Table S1). Two hundred nanograms of purified PCR product was annealed according to the following settings: 95 °C for 5 min and ramp down to 25 °C (at 0.5 °C/min). The annealed product was then treated with T7 endonuclease (New England Biolabs, Ipswich, MA, USA) at 37 °C for 30 min and separated on 1% agarose gel. Related indels were detected using the TanonMP gel imaging system (Tanon, Shanghai, China) and sgRNA indel efficiency was calculated using ImageJ software (NIH, Bethesda, MD, USA).

Stable cell lines generation

Cells were stably transfected with different donor plasmids and/or sgRNA plasmids. For CHO-K1 cells, 8 µg/mL of puromycin (Amresco, Solon, OH, USA) was used for 2 weeks and 50 µg/mL *Lens culinaris* agglutinin (LCA) (Vector

Laboratories, Peterborough, UK) for an additional week to enrich integrated cells. For CHO-S cells, 8 µg/mL puromycin was used for 3 weeks. Stably transfected pools were then detected with 5'/3' junction PCR and Western blot, and further seeded at 0.5–1 cell/well in 96-well plates for limiting dilution. After another 3–4 weeks, the colonies were generated and analyzed by 5'/3' junction PCR and Western blot for protein expression. Only those colonies positive in both junction PCR and Western blot assessment were selected for further investigation.

Genomic DNA extraction and 5'/3' junction PCR at target region

Genomic DNA was extracted with QuickExtract DNA extraction solution (Epicenter, Madison, WI, USA) from stably transfected pools and single cell clones for the amplification of 5'/3' junction PCR according to the following PCR procedure: 94 °C for 2 min; 30×: 94 °C for 30 s, 65 °C–50 °C (–0.5 °C/cycle) for 30 s, 72 °C for 2 min; 20×: 94 °C for 30 s, 50 °C for 30 s, and 72 °C for 2 min. Primers are listed in Supplementary Table S1. Purified 5'/3' junction PCR product was sequenced by Invitrogen.

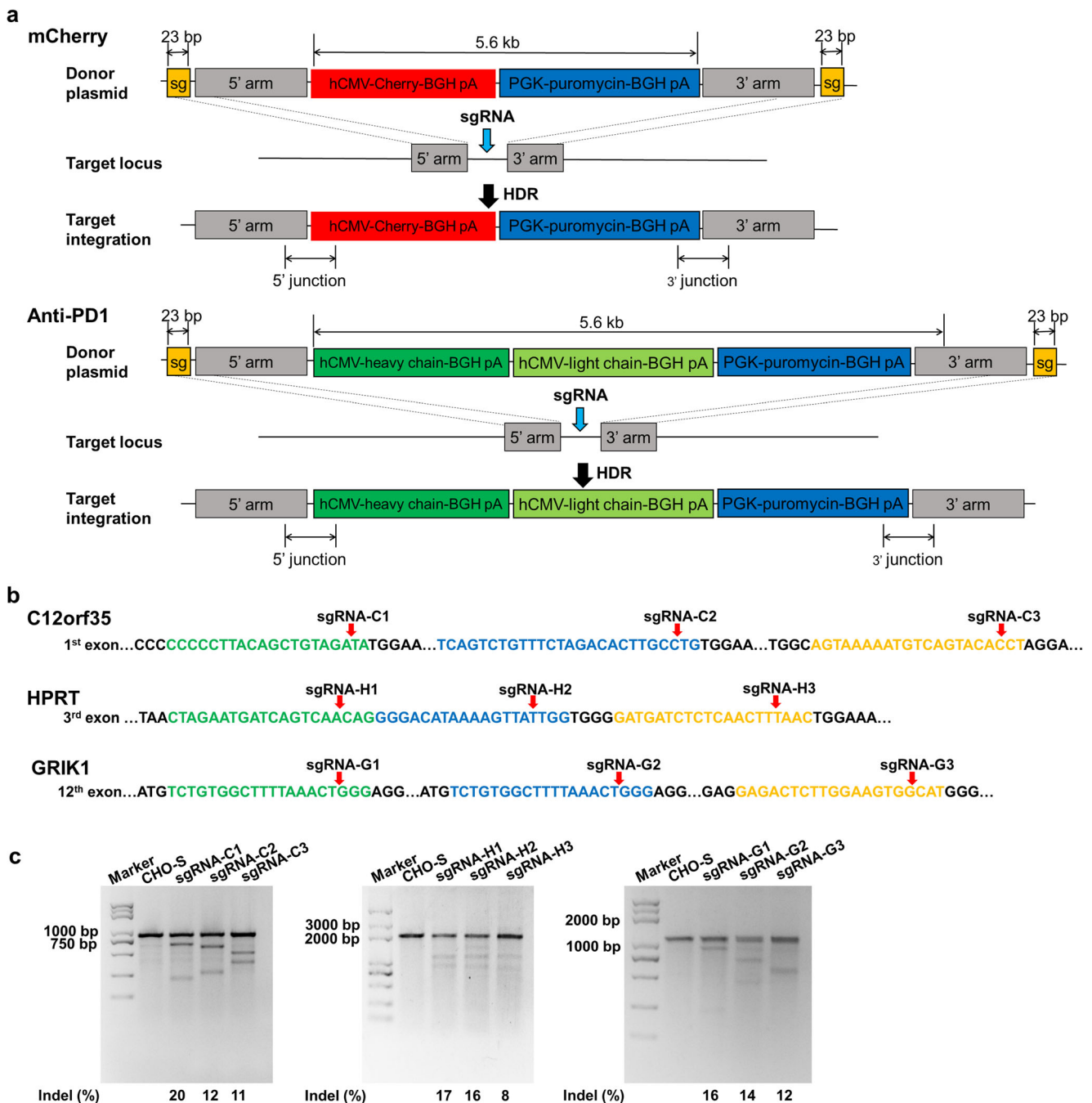


Fig. 2 Screening of efficient editing sgRNAs and construction of donor plasmids for three candidate integration sites. **a** Schematic diagram of HDR-mediated site-specific integration. Donor plasmids were constructed with 5'/3' homology arms (750 bp), the protein-encoding gene (mCherry or anti-PD1 mAb), CRISPR target sites (sg, 23 bp), and resistance gene (puromycin). As sgRNA-Cas plasmids were transfected into CHO-S cells, donor plasmids were introduced to linearize DSB breaks at the predetermined site. HDR-mediated repair was inserted into the DSB location to achieve targeted integration. **b** The locations of three sgRNAs

targeting their respective integration sites. SgRNAs designed for the C12orf35 locus was concentrated in the 1st exon. Targeted HPRT locus were distributed at the 3rd exon and targeted GRIK1 gene was spread throughout the 12th intron. **c** T7EI endonuclease assay for detection of Cas9 editing activity in CHO-S cells. Three days after transfection of CHO-S cells with different Cas9 editing plasmids, the three respective sites were assessed by PCR amplification of genomic DNA. Two hundred nanograms of PCR product was loaded onto each lane

Detecting targeted protein expression

After identification by 5'/3' junction PCR, positive clones were further analyzed for expression titer by flow cytometry

or Western blot, respectively. For mCherry, 1×10^6 cells of each clone were washed with PBS and re-suspended in 500 μ L PBS for flow cytometry analysis. For CTLA4Ig and anti-PD1 mAb, the cells supernate were collected and

separated by a 10% SDS-PAGE. Next, the protein was transferred to a 0.45- μ m PVDF membrane, which was blocked by 10% skim milk, and then incubated with HRP conjugated Affinipure donkey anti-human IgG (H+L) antibody (Jackson ImmunoResearch Laboratories, Inc., Baltimore, PA, USA) to recognize target proteins. The bands recognized by the antibody were detected by Immobilon Western Chemiluminescent HRP Substrate (Millipore, Billerica, MA, USA) and visualized with the TanonMP gel imaging system (Tanon, Shanghai, China).

Quantitative real-time PCR for copy number analysis

To determine the relative copy number of the genes encoding mCherry and anti-PD1 mAb, FastStart Universal SYBR Green Master (Roche, Mannheim, Germany) was used to prepare samples in triplicate on Applied Biosystems StepOnePlus Real-time PCR System (Thermo Fisher Scientific, Waltham, MA, USA) with the following parameters: 95 °C for 10 min; 40 \times : 95 °C for 15 s, 60 °C for 60 s. All primers were designed for transgene analysis including mCherry and anti-PD1 mAb, with target genes including C12orf35, HPRT, GRIK1 (sgRNA-C1, sgRNA-H1, and sgRNA-G1 target site, respectively), and reference gene GAPDH (Supplementary Table S1). The delta-delta threshold cycle ($\Delta\Delta C_T$) method was used to calculate relative copy numbers of targeted genes (C12orf35, HPRT, GRIK1) related to endogenous products in wild-type CHO-S cells, and that of transgenes (mCherry, anti-PD1 mAb) related to reference clones obtained by random integration.

Determination of exogenous protein productivity and cell line stability

The productivity of mCherry-expressing stable cell lines was determined by flow cytometry. The production levels of anti-PD1 mAb stable cell lines were evaluated by the final mass of antibodies purified by a prepacked MabSelect SuRe column (GE Healthcare, Uppsala, Sweden). In detail, the column was balanced with binding buffer (20 mM phosphate buffer with 150 mM NaCl, pH 7.4) for five column volumes (CVs). Then the culture supernatant was loaded on the column at a rate of 1 mL/min, and the product was eluted with elution buffer (100 mM citric acid buffer, pH 3.0), which was immediately adjusted to pH 7.0 by adding 1 M Tris-HCl buffer (pH 9.0). The elutants containing target antibodies were dialyzed with a 25-kDa dialysis bag in PBS and subsequently quantified by BCA Protein Assay Kit (Beyotime, Shanghai, China). Furthermore, the stability of the cell lines was assessed by culturing the cells for 20 passages and performing purification and evaluation every five passages.

Binding affinity measurement

The binding affinity of anti-PD1 mAbs was determined by Surface Plasmon Resonance (SPR) using BIAcore T200 (GE Healthcare, Uppsala, Sweden). Recombinant human PD1-His protein (encoding the extracellular domain of human PD1 with amino acids Met 1 to Gln 167; Sino Biological Inc., Beijing, China) was coated on a CM5 sensor chip, with PBS with 0.1% Tween 20 as running buffer. Binding rate (K_a), dissociation rate constants (K_d), and the equilibrium dissociation constant (K_D) were determined using a binding model with concentration series adjusted to a 1:1.

Glycosylation analysis by LC-FLR-MS

LC-FLR-MS method was used to analyze glycosylation of anti-PD1 antibodies produced by the selected stable clones. According to GlycoWorks RapiFluor-MS N-Glycan Kit Care and Use manual (Waters, Milford, MA, USA), 7.5 μ L of purified antibody (1 mg/mL) was mixed with 15.3 μ L of 18.2 M Ω water and 6 μ L of 5% RapiGest SF Surfactant solution, followed by denaturation at 95 °C for 5 min. After cooling down to room temperature, 1.2 μ L of Rapid PNGase F was added to release the N-linked glycans from the antibody, and 12 μ L of RMFS solution was added to each N-linked glycan sample for labeling N-glycosylamine, which were further purified by hydrophilic interaction chromatography (HILIC) column. Finally, the prepared samples were loaded on a Waters Acquity ultrahigh-performance liquid chromatography I class system (UPLC) was equipped with FLR detector. UPLC BEH Glycan column (2.1 mm \times 150 mm) was used with mobile phases A and B (A: 50 mM ammonium formate, pH 4.4; B: 100% acetonitrile) to separate oligosaccharides, which were further precisely identified by an interfaced Waters VION IMS Quadrupole time-of-flight mass spectrometer (QTOF).

Analysis of off-target effects by whole-genome sequencing for high-expressing clones

Clones KP6 and KP11 harboring anti-PD1 mAbs at the C12orf35 locus showed a high level of productivity and stability, indicating the site is a potential integration hot spot. Therefore, we performed whole-genome sequencing of the two clones to assess potential off-target mutations induced by CRISPR/Cas9. Two micrograms of genomic DNA for each clone was sheared to 400 bp fragments for the construction of an Illumina PE sequencing library and then sequenced on Illumina PE 150 platform with 60 Gbp clean data. Sequencing data were compared with the reference genome of CHO cell line (genome ID: 2791) acquired from NCBI through BWA, GATK, and BreakDancer software. The

Illumina sequencing raw data of clones KP6 and KP11 have been deposited in NCBI Sequence Read Archive database (SRA accession number for clone KP6: SRP129928, SRA accession number for clone KP11: SRP128889).

Results

Method establishment for site-specific integration in CHO cell lines using CRISPR/Cas9

To investigate possible transcriptional hot spots in CHO cells, we assessed the feasibility of CRISPR/Cas9-mediated site-specific integration by targeting CTLA4Ig gene into the FUT8 locus in CHO-K1 cells. Firstly, we screened two most efficient sgRNA (editing efficiency with 27.5% for sgRNA 2 and 31.7% for sgRNA 5) to double-click the *FUT8* loci as shown in Fig. 1a and b. After transfection, a stable cell pool was generated by puromycin selection for 2 weeks and enrichment by LCA for an additional week. The 5'/3' junction PCR results indicated that transfected pools co-transfected with sgRNA vectors and donor plasmids could be amplified for the target band of 1200 bp, which was not observed in random transfected pools (Fig. 1c). Further sequencing confirmed the precise gene insertion at FUT8 locus (Supplementary Fig. S1). After limited dilution for selection, we obtained 56 single clones, among which 21 clones were 5'/3' junction PCR positive and adequately expressed the target protein (Fig. 1d). These results demonstrated that this site-integration method through CRISPR/Cas9 technology was applicable for subsequent study.

Site-specific integration and plasmid construction, sgRNAs design and screening

To explore the most efficient integration sites, we constructed plasmids as shown in Fig. 2b to insert the expressing cassettes into the chromosomes of CHO-S cells. Donor plasmids carrying mCherry and anti-PD1 genes were constructed due to their ease of detectability or monoclonal nature (the most prevalent type of biopharmaceuticals). According to previous studies, linear fragments were favorable for HDR in comparison to circular plasmids (Irion et al. 2014). Therefore, we constructed the donor plasmids with 5' and 3' homology arms flanked by the above selected sgRNA sequences and to linearize the insertion fragment, thus improving the efficiency of HDR-mediated targeted integration. Three sgRNAs for each targeting site were designed and assessed by T7EI endonuclease assay. As shown in Fig. 2c, the most efficient sgRNAs were identified to be sgRNA C1, sgRNA H1, and sgRNA G1. They were used to transfect CHO-S cells and mediate Crispr/Cas9-assisted site-specific integration by HDR.

Selection and identification of targeted stable cell clones

After transfection, we extracted genomic DNA and performed 5'/3' junction PCR, which showed desired fragments in agarose gel analysis (Supplementary Fig. S2). The sequencing of the amplified PCR fragments further confirmed that there was a successful insertion of exogenous genes (mCherry, anti-PD1 mAb) into all the three target sites (Supplementary Fig. S3 A–F). However, according to protein expression detected by flow cytometry or Western blot, there was no difference observed between random and targeted integration transfected pools 3 days post transfection for either mCherry or anti-PD1 mAb (Fig. 3a, b). It can be explained that target proteins were mainly from transient expression at 3 days post transfection, which overwhelming the low percentage of integrated stable expression.

In the stably transfected pools after 3 weeks of puromycin selection, all targeted integration showed higher levels of protein expression compared to random integration cells for both mCherry and anti-PD1 mAb transfected pool (Fig. 3c, d). Additionally, we analyzed protein production. For mCherry, C12orf35 targeted pool displayed a 4-fold higher expression compared to HPRT targeted pool, 6-fold higher than GRIK1 targeted pool and 18-fold higher than random integration pool (Supplementary Fig. S4 A–D). For anti-PD1 mAb, C12orf35 targeted pool displayed a 2-fold higher expression compared to HPRT targeted pool, 3-fold higher than GRIK1 targeted pool and a 9.5-fold higher than the random integration pool (Supplementary Fig. S5 A–D). In summary, the results indicated that C12orf35 locus could be a promising transcriptional hot spot for exogenous gene expression.

After verification of transfected pools expression, limiting dilution was used to obtain the targeted cell clones, which were further verified by 5'/3' junction PCR for positive clones. For mCherry expressing clones, 21 out of 35 single clones for C12orf35 locus targeted integration (Supplementary Fig. S6 A and B), 46 out of 95 for HPRT locus (Supplementary Fig. S7 A and B), and 31 out of 47 for GRIK1 locus (Supplementary Fig. S8 A and B) were confirmed for successful integration. For anti-PD1 mAb expressing clones, 10 out of 24 single clones for C12orf35 locus (Supplementary Fig. S9 A and B), 17 out of 48 for HPRT locus (Supplementary Fig. S10 A and B), and 15 out of 63 for GRIK1 locus (Supplementary Fig. S11 A and B) were confirmed for successful integration. We then used flow cytometry and Western blot analysis to verify the expression of targeted proteins (mCherry, anti-PD1 mAb) for 5'/3' junction PCR positive clones, and all clones were confirmed to express target genes successfully (Supplementary Fig. S12 A–C and Fig. S13 A–C). The results demonstrated that all of the three selected sites could be used for site-specific integration of exogenous genes with the targeting efficiency of 48.4–66% for recombinant proteins like mCherry or 25.4–41.7% for IgG protein like anti-PD1 mAb (Fig. 3e).

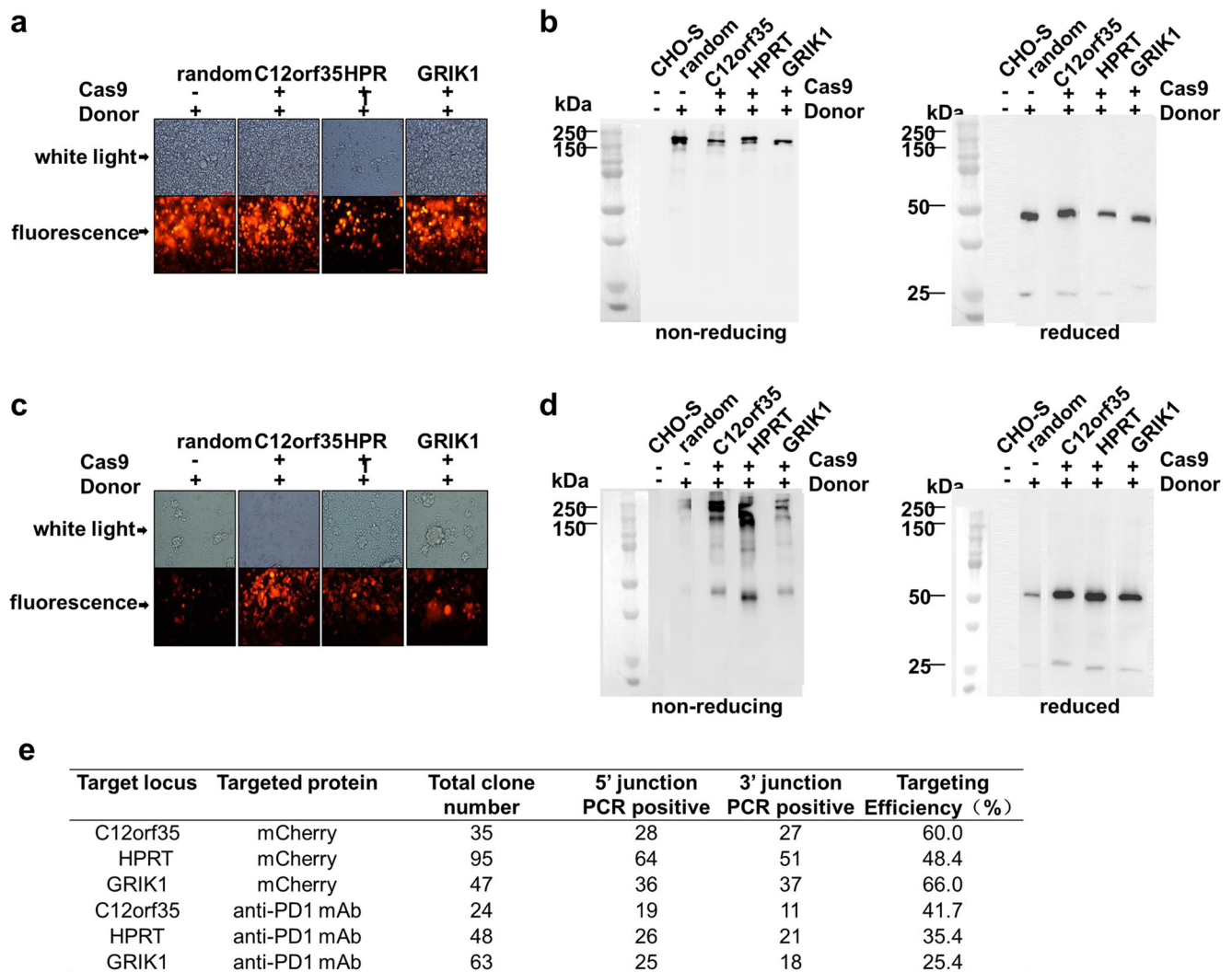


Fig. 3 Expression of targeted protein after transfection and puromycin selection and targeting efficiency of stable cell clones. **a** mCherry expressing transfected pools were verified by inverted fluorescence microscope 3 days after transfection. **b** Anti-PD1 mAb expressing transfected pools were verified by Western blot 3 days after transfection. The left figure represents non-reduced protein while right represents reduced protein. **c** mCherry expressing transfected pools were detected after puromycin selection for 3 weeks. **d** Anti-PD1 mAb expressing

transfected pools were detected after puromycin selection for 3 weeks. The left figure indicates non-reducing samples while right indicates reduced samples. Random transfected pools were obtained by transfection of mCherry or antibody donor plasmid only, while site-specific integration transfected pools were obtained by transfection of mCherry or antibody donor plasmid plus Cas9 editing plasmid. **e** Targeting efficiency of stable cell clones. Targeting efficiency was obtained by the percentage of 5'/3' junction PCR positive clones among total clones investigated

Growth profile, relative copy number, and productivity analysis in targeted integration clones

To investigate the loci for their potential application in site-specific integration, we randomly selected two stable clones for each site to perform further analysis. For C12orf35 targeted clones, we selected KC6 and KC15 for mCherry and KP6 and KP11 for anti-PD1 mAb integration. For HPRT targeted clones, we selected HC6 and HC18 for mCherry and HP8 and HP38 for anti-PD1 mAb integration. For GRIK1 targeted clones, we selected GC1 and GC7 for mCherry and GP34 and GP58 for anti-PD1 mAb integration. Additionally, we cultured randomly

integrated clones as controls including one clone RC16 for mCherry, and two clones RRP21 and RP26 for anti-PD1 mAb expression. We then compared the cell growth curves of targeted clones with wild-type clones (CHO-S) for three parallel experiments. As shown in Fig. 4a, b, growth profiles of stable cell clones overall showed no significant difference concerning the transgene insertion sites. All the three studied sites are not essential to cell growth and could be engineered without substantial interference to cell characteristics.

The transcripts of the integration sites and exogenous genes in targeted integration clones were analyzed by real-time RT-PCR. For clones KC6, HC6, HC18, GC1, KP6, KP11, HP8, HP38, and GP34, the ratios of insertion site copy numbers relative to the

sites in wild-type CHO-S cells were close to 0, indicating a nearly complete disruption in these targeted cell clones (Fig. 5a–h). While clones KC15, GC7, and GP58 had a partial number of relative insertion copy number, suggesting monoallelic knock-in that induced heterozygous disruptions in these clones (Fig. 5c, e, h). For mCherry expressing clones, GC1 had the highest relative mCherry copy number (about four copies while other clones with only one copy) (Fig. 5a). For anti-PD1 mAb expressing clones, KP6, KP11, and RP26 had higher relative antibody copy numbers (3–4 copies) than other clones (1 copy) (Fig. 5b). To summarize the data, mRNA expression level of the inserted gene was not dependent on integrated locus or biallelic/monoallelic insertion, indicating all three studied loci suitable for stable transcription of the exogenous gene.

Expression stability of clones with targeted integration

We further assessed the site-specific integration strategy by evaluation of rCHO cell lines productivity and stability. The cell lines were cultivated for a total of 20 passages and the expressing level was inspected every five passages. For mCherry integrated cells, KC6 and KC15 at C12orf35 locus maintained expression level of 10,000–20,000 RFU, while productivity of other clones began to decrease after the 10th passage (Fig. 6a) (Supplementary Fig. S14 A–G). For anti-PD1 mAb integrated cells, KP6 and KP11 exhibited stable productivity of 110–190 mg/L for over 20 passages. Meanwhile, productivities of all other selected clones were much lower with an average level of 6.15 ± 3.64 mg/L for passage 5. What is more, clones HP38 and RP21 even failed to grow over 15 passages, indicating the un-stability of the two cell lines (Fig. 6b) (Supplementary Fig. S15 A–H).

We further investigated the productivity of anti-PD1 mAb of pg/cell/day. As shown in Fig. 6c, KP6 and KP11 showed dramatically higher production ability compared to clones integrated into other sites, which reached up to 10–13 pg/cell/

day and was sustained during 20 passages, supporting that C12orf35 is an ideal integration target for exogenous gene expression. All the above data demonstrated that C12orf35 targeted integration is a promising strategy for establishing recombinant clones with high and stable productivities for biopharmaceutical manufacturing.

Quality assessment of the products produced by targeted integrations

We analyzed the antigen binding affinity and glycosylation of anti-PD1 mAbs to evaluate the quality of the products produced by site-specific integrated cells of passage 5 and passage 20. As shown in Table 1, K_D for KP6 and KP11 at C12orf35 locus fell between 1.64 and 2.82, for HP8 it was between 2.54 to 4.03, and for GP34 it was between 1.85 and 3.06 (Supplementary Fig. S16 A–D). The overall affinity of anti-PD1 mAbs generated from all targeted integration clones was identical to previously published reports (Ding et al. 2017; Wang et al. 2014).

Glycosylation is among the most critical quality control criteria for monoclonal antibody drugs. To explore the effect of integrated sites on glycosylation, we analyzed the N-glycan patterns of anti-PD1 mAbs produced. As shown in Table 2, all the products produced by selected cell lines showed similar N-glycosylation patterns, without significant relationship to cell passages (passages 5 and 20). The results illustrated that the detected three integration sites did not affect glycosylation and were suitable for exogenous protein producing. All the above data demonstrated that the cell lines developed by site-specific integration could produce products with stable quality for at least 20 passages.

Off-target assessment

The off-target effect is always a concern for application of CRISPR/Cas9 technology. Here we analyzed the off-target mutations of KP6 and KP11 by whole-genome sequencing, which

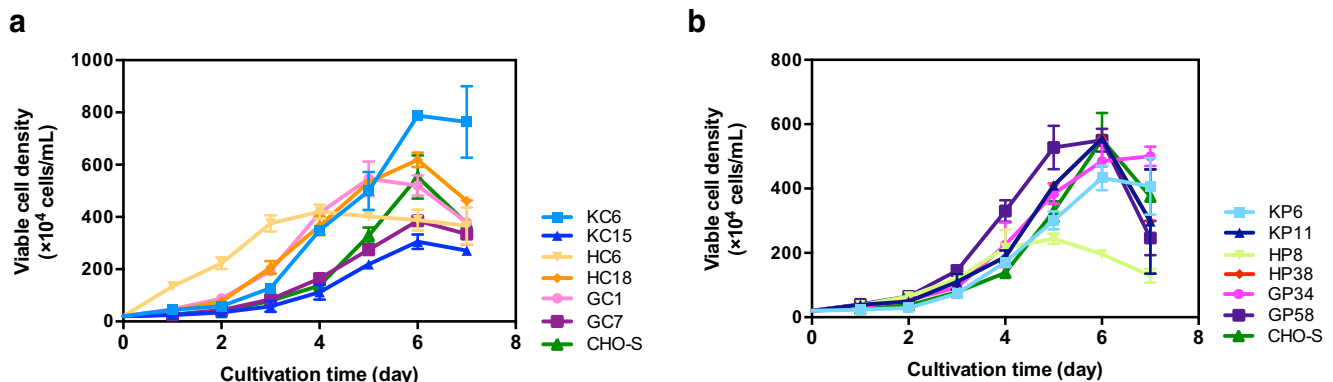


Fig. 4 Cell growth curves and productivity of selected transgene cell lines. **a** Cell growth of mCherry expressing clones and CHO-S. **b** Cell growth of anti-PD1 mAb expressing clones and CHO-S. Cell density was

tested in 125-mL shaker flasks with 20 mL culture medium after 8 days of cultivation. The error bars represent standard deviation (SD) of three parallel experiments

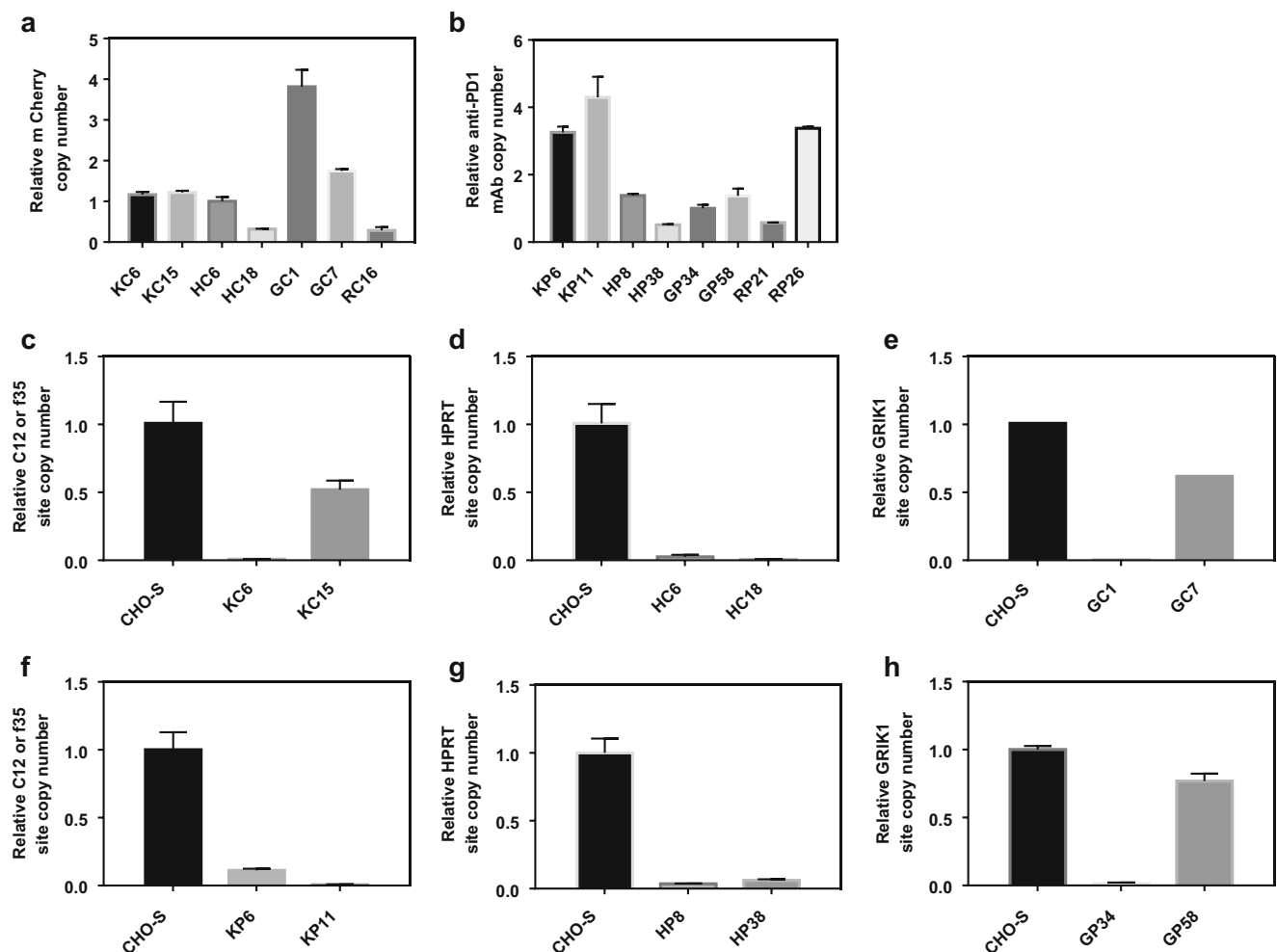


Fig. 5 Relative copy numbers of insertion sites and targeted exogenous genes in integrated clones. **a, c–e** Relative copy number for mCherry expressing clones. **b, f–h** Relative copy number for anti-PD1 mAb expressing clones. Genomic DNA of wild-type CHO-S was used as the reference

for calculating relative insertion site copy number, Clone HC6 was used as the reference for measuring relative mCherry copy number, and Clone GP34 was used as the reference for measuring relative antibody copy number. The error bars represent the standard deviations ($n = 3$)

with improved integrity, accuracy, and randomness for sequencing detection (Fig. 7a). According to data analysis, GC percentages for both clones were about 41% (Fig. 7b). There were totally 58 mutations for KP6 and 59 for KP11 identified and classified into Stopgain (early termination), Stoploss (terminator missing), Frameshift deletion/insertion/substitution, and Non-frameshift deletion/insertion/substitution (Fig. 7c). Since the median protein code for CHO cell is 32,843 (data from National Center for Biotechnology Information, NCBI), the off-target efficiency was calculated to be 0.17% for clone KP6 and 0.18% for clone KP11. Despite these mutations, both clones were stable in cell growth and productivity during the cultivation of 20 passages, indicating that off-target mutations induced by CRISPR/Cas9 did not contribute to cell properties or exogenous genes expression. C12orf35 locus targeted integration mediated by CRISPR/Cas9 was a reliable and high efficient strategy to develop rCHO cell lines for industrial application.

Discussion

In this study, we identified a transcriptional hot spot C12orf35, with which we set up a CRISPR/Cas9-mediated site-specific integration strategy to rapidly develop stable transgene cell lines for biopharmaceutical industrial applications. Using this approach, we successfully obtained stable cell lines to produce mCherry and anti-PD1 mAb with excellent cell stability and productivity.

CRISPR/Cas9 is a powerful technology for engineering CHO cells to satisfy biopharmaceutical research demands. It was employed to establish FUT8 knockout CHO-S cells in our previous work which produced defucosylated antibodies with enhanced in vitro antibody-dependent cellular cytotoxicity (Sun et al. 2015; Zong et al. 2017). Site-specific integration of exogenous genes into CHO cells through CRISPR/Cas9 was also discussed, even though no pharmaceutical purposed application was performed (Lee et al. 2015). Here we aimed to

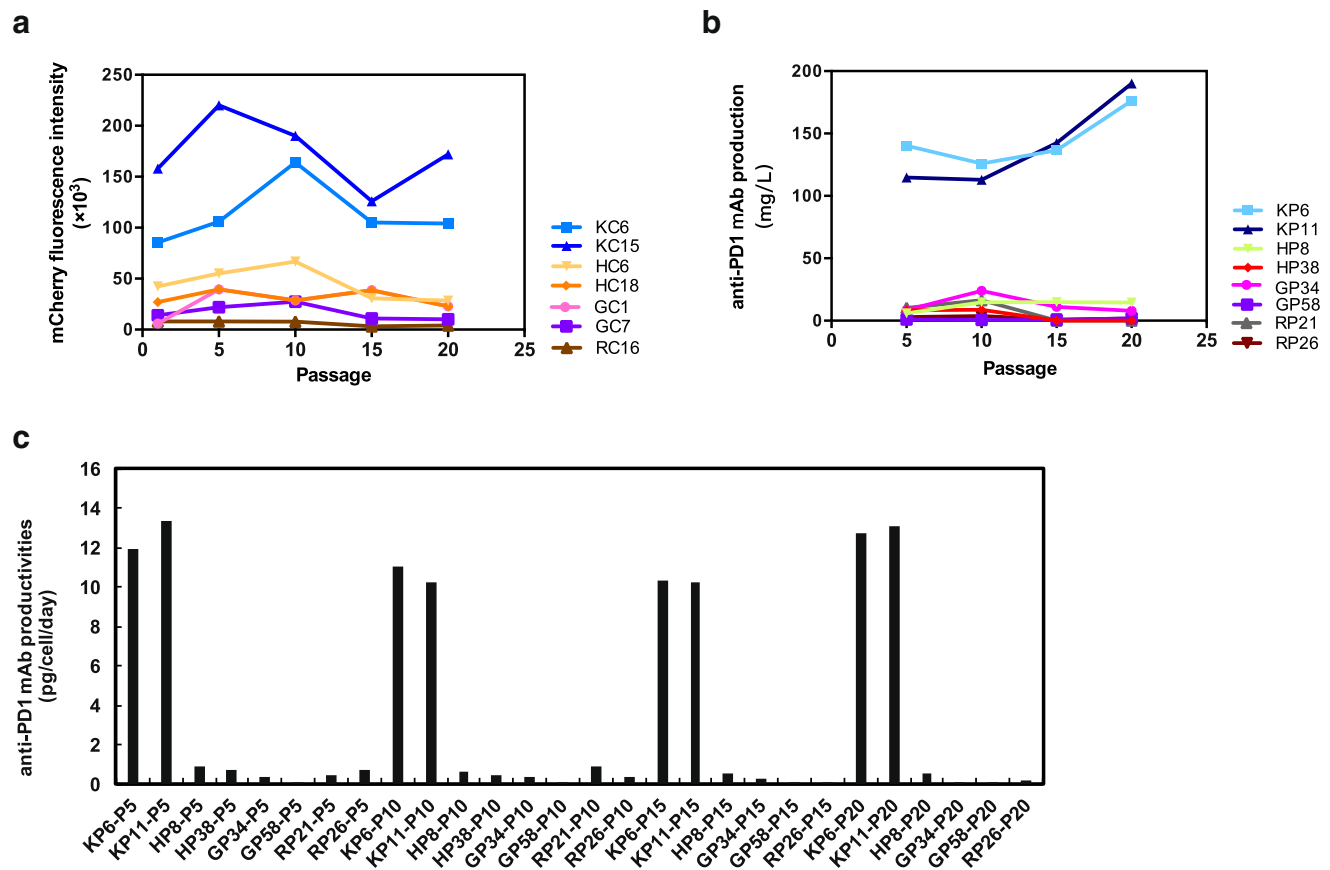


Fig. 6 Production of targeted protein for stable cell clones during long-term cultivation. Two clones were selected for each integration site to determine the productivity of mCherry (**a**) or anti-PD1 mAb (**b**) for over 20 passages. Randomly selected clones RC16 and RP21, RP26 were used as control. C12orf15 integrated KC6, KC15, KP6, KP11 showed

significantly higher and stable productivity in comparison with other sites integrated clones. **c** Anti-PD1 productivity (pg/cell/day) and sustainability of the selected clones. KP6 and KP11 showed dramatically higher productivities as well as exemplary sustainabilities for over 20 passages's cultivation

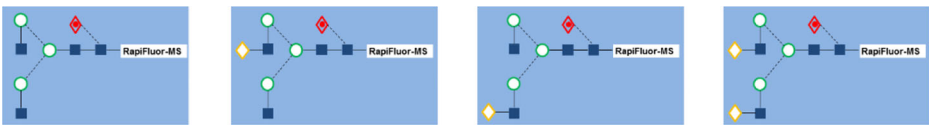
use CRISPR/Cas9-mediated site-specific integration to determine potential high transcriptional active sites in CHO cells, to improve the development process of stable cell lines for industrial applications. We first demonstrated the feasibility of this strategy by inserting CTLA4Ig into FUT8 locus in CHO-K1 cells. Then we investigated three candidate chromosomal positions (C12orf35, HPRT, GRIK1) for targeted

integration of two representative model proteins (mCherry, anti-PD1 mAb) in experimental CHO-S cells. To optimize the strategy, we added two sgRNA sequences flanking the insertion fragments for the donor plasmid to linearize the exogenous genes during the transfection process. The method improved the targeting efficiency from reported 10–30% to our 25.4–66.0% with precise integration of exogenous genes (from 3.7 to 5.9 kb) at targeted sites (Fig. 2) (Lee et al. 2016; Lee et al. 2015).

Productivity and stability are the two most crucial factors in stable cell line development. As observed during multi-passage cultivation, the stable cell lines integrated at C12orf35 locus resulted in the highest productivity and stability compared to the random cells and other targeted integration cells for both mCherry protein and anti-PD1 mAb. Notably, the mCherry integrated clones at C12orf35, KC6 and KC15, displayed 50-fold higher expression level than HPRT, GRIK1, or random integrated clones. The anti-PD1 mAb integrated clones at the C12orf35 site, KP6 and KP11, displayed a 10-fold higher expression level than other site integrated clones and random integrated clones. Moreover, the levels of

Table 1 K_a , K_d , and K_D of anti-PD1 mAbs produced by integrated clones

Sample	K_a (1/Ms)	K_d (1/s)	K_D (nM)
KP6-P5	3.25×10^5	7.11×10^{-4}	2.19
KP11-P5	2.79×10^5	4.58×10^{-4}	1.64
HP8-P5	2.58×10^5	6.54×10^{-4}	2.54
GP34-P5	2.71×10^5	5.00×10^{-4}	1.85
KP6-P20	3.41×10^5	9.61×10^{-4}	2.82
KP11-P20	3.56×10^5	7.31×10^{-4}	2.05
HP8-P20	2.23×10^5	9.00×10^{-4}	4.03
GP34-P20	1.88×10^5	5.74×10^{-4}	3.06

Table 2 N-glycan patterns of anti-PD1 mAbs produced by stable clones of different integrated sites


%	G0F	G1F	G1F	G2F
KP6-P5	57.65	16.00	14.57	7.26
KP11-P5	65.47	13.34	11.97	5.11
HP8-P5	56.38	16.04	13.75	7.35
GP34-P5	66.41	10.49	9.39	4.49
KP6-P20	62.39	11.62	10.82	4.62
KP11-P20	70.65	8.94	8.30	3.66
HP8-P20	71.07	10.35	9.02	3.15
GP34-P20	75.04	8.87	8.53	3.98

* ■ N-acetyl glucosamine ○ mannose ◇ galactose ◆ fucose

mCherry protein in KC6 and KC15 clones and anti-PD1 mAb in KP6 and KP11 clones held stable for 20 passages. These results demonstrated that exogenous gene induction into the

C12orf35 locus could maintain the producing level and cell stability for at least 20 passages, strongly suggesting that the C12orf35 locus is a transcriptional hot spot in CHO cell lines.

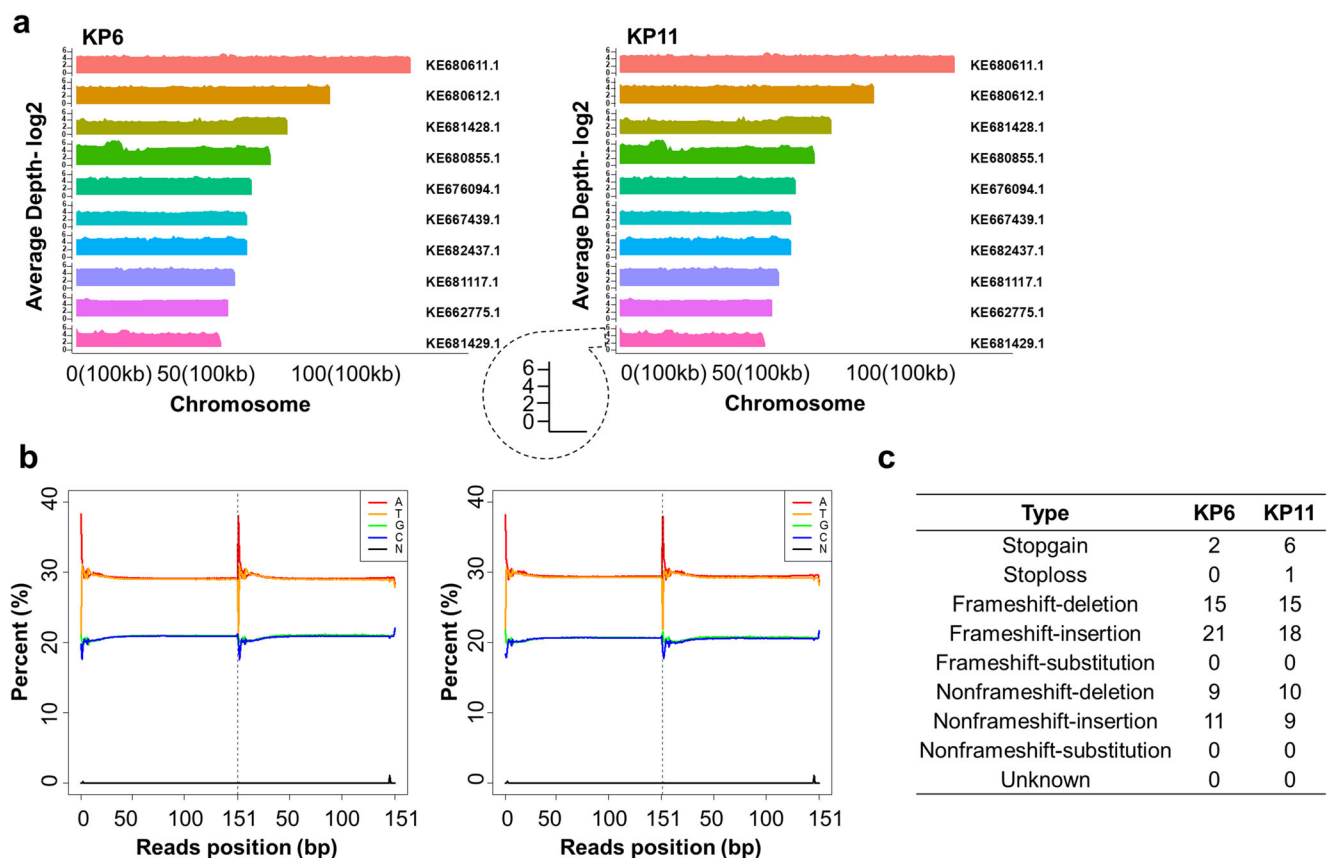


Fig. 7 Off-target assessment by whole-genome sequencing on Illumina PE 150 platform for clones KP6 and KP11. **a** Covering depth distribution map of the chromosome for Illumina sequencing. **b** Base distribution for high-expressing cell clones. **c** Summary of identified off-target mutations. Stopgain, early termination of locus mutations; stoploss, terminator missing; frameshift-deletion, frameshift mutations induced by lacking of

bases; frameshift-insertion, frameshift mutations induced by base insertion; frameshift-substitution, frameshift mutations induced by base substitution; non-frameshift-deletion, non-frameshift mutations induced by deletion; non-frameshift-insertion, non-frameshift mutations induced by insertion; non-frameshift-substitution, non-frameshift mutations induced by substitution

One of the limitations of this study was that the current productivity data was drawn from shake flasks cell culture rather than from bioreactors. Expression of recombinant proteins in a bioreactor would be more representative of the industry applications and which should be further examined.

Our strategy to insert exogenous genes into the C12orf35 locus of CHO cells through CRISPR/Cas9 significantly improved the efficiency to develop stable transgene cell lines. Multiple rounds of pressure selection were usually necessary to construct rCHO cell lines of high yields by conventional random integration strategy (~6–12 months) (Lai et al. 2013). Both of time and cost could be saved if using the site-specific integration strategy here reported, which takes only 3 weeks to get targeted transfected pools and 5 weeks to select integrated clones. However, with current process there was just ~200 mg/L productivity for anti-PD1 mAb, which is far away from meeting the industrial demands. Considering the low cell density (~ 3×10^6 /mL) and sub-optimal conditions in shake flasks, it is promising to improve productivity by 5–10-folds through optimization of cell culture conditions, including media, supplements, dissolved oxygen, trace elements, or even using perfusion fed-batch process (Hiller et al. 2017; Xu and Chen 2016). On the other hand, cell biology-based strategies can further improve target protein production, such as key molecules for cell cycle, apoptosis, or metabolism (Josse et al. 2016; Templeton et al. 2014).

Off-target effect induced by CRISPR/Cas9 is the main obstacle for this site-specific integration method. It has been reported that base-mismatch of sgRNA may be the principal contributor to off-target mutations (Cong et al. 2013; Mali et al. 2013). Many researchers have previously assessed target specificity by identifying potential off-target sites for each sgRNA edit sequence (Lee et al. 2015). Unfortunately, the predicted off-target mutations may not entirely coincide with actual mutations. In this report, we used whole-genome sequencing to thoroughly evaluate the impacts of protein translation induced by off-targeted mutations. Fortunately, all detected off-target mutations were limited to two clones, KP6 and KP11, and did not affect cell growth or antibody expression. In the future, several other approaches can be used to improve on-target specificity, such as the design of highly efficient sgRNAs (Doench et al. 2016; Moreno-Mateos et al. 2015), employing high-fidelity SpCas9 (Kleinstiver et al. 2016), or reducing off-target activity through double nicking (Ran et al. 2013).

Improving the efficiency, productivity, and stability during cell line development has always been a challenge for research and industrial manufacturing. In this study, we identified an ideal integration site C12orf35, and developed a reliable site-specific integration strategy mediated by CRISPR/Cas9 to establish stable cell lines of high productivity and excellent stability. Due to the wide use of CHO cells for mAb drugs production, the integrated gene for anti-PD1 mAb could hypothetically be substituted by other antibodies to develop stable

cell clones for target drug production. In addition, there have been some other valuable techniques developed for recombinant cell line development, such as the AGIS system which can accumulate an expression cassette to improve target protein productivity (Wang et al. 2017) or the high-efficiency CRIS-PITCH system which requires much shorter and simpler microhomology sequences for targeting (Kawabe et al. 2017). The combination of these advanced strategies could be applied to develop cell lines with high productivity, stability, and efficiency for biopharmaceutical industrial purposes.

Acknowledgements We would like to thank Dr. Xiangping Zhu, Yuan Gao, and Man Wang at Jecho Biopharmaceuticals Co., Ltd. in Tianjin, China, for professional help in quality analysis of the monoclonal antibodies.

Funding This work was supported in part by the National Natural Science Foundation of China (No. 81273576, 81773621) and the Science & Technology Commission of Shanghai Municipality (No. 15431907000 and 17431904500).

Compliance with ethical standards

Conflict of interest Authors declare that they have no conflict of interest.

Ethical approval This article does not contain any studies with human participants or animals experiments.

References

- Bachu R, Bergareche I, Chasin LA (2015) CRISPR-Cas targeted plasmid integration into mammalian cells via non-homologous end joining. *Biotechnol Bioeng* 112(10):2154–2162. <https://doi.org/10.1002/bit.25629>
- Baser B, Spehr J, Bussow K, van den Heuvel J (2016) A method for specifically targeting two independent genomic integration sites for co-expression of genes in CHO cells. *Methods* 95:3–12. <https://doi.org/10.1016/j.ymeth.2015.11.022>
- Cheng JK, Lewis AM, Kim do S, Dyess T, Alper HS (2016) Identifying and retargeting transcriptional hot spots in the human genome. *Biotechnol J* 11(8):1100–1109. <https://doi.org/10.1002/biot.201600015>
- Cong L, Ran FA, Cox D, Lin S, Barretto R, Habib N, Hsu PD, Wu X, Jiang W, Marraffini LA, Zhang F (2013) Multiplex genome engineering using CRISPR/Cas systems. *Science* 339(6121):819–823. <https://doi.org/10.1126/science.1231143>
- Damavandi N, Raigani M, Joudaki A, Davami F, Zeinali S (2017) Rapid characterization of the CHO platform cell line and identification of pseudo *attP* sites for PhiC31 integrase. *Protein Expr Purif* 140:60–64. <https://doi.org/10.1016/j.pep.2017.08.002>
- Ding K, Han L, Zong H, Chen J, Zhang B, Zhu J (2017) Production process reproducibility and product quality consistency of transient gene expression in HEK293 cells with anti-PD1 antibody as the model protein. *Appl Microbiol Biotechnol* 101(5):1889–1898. <https://doi.org/10.1007/s00253-016-7973-y>
- Doench JG, Fusi N, Sullender M, Hegde M, Vaimberg EW, Donovan KF, Smith I, Tothova Z, Wilen C, Orchard R, Virgin HW, Listgarten J, Root DE (2016) Optimized sgRNA design to maximize activity and

- minimize off-target effects of CRISPR-Cas9. *Nat Biotechnol* 34(2): 184–191. <https://doi.org/10.1038/nbt.3437>
- Fischer S, Handrick R, Otte K (2015) The art of CHO cell engineering: a comprehensive retrospect and future perspectives. *Biotechnol Adv* 33(8):1878–1896. <https://doi.org/10.1016/j.biotechadv.2015.10.015>
- Galleguillos SN, Ruckerbauer D, Gerstl MP, Borth N, Hanscho M, Zanghellini J (2017) What can mathematical modelling say about CHO metabolism and protein glycosylation? *Comput Struct Biotechnol J* 15:212–221. <https://doi.org/10.1016/j.csbj.2017.01.005>
- Gupta SK, Shukla P (2017) Gene editing for cell engineering: trends and applications. *Crit Rev Biotechnol* 37(5):672–684. <https://doi.org/10.1080/07388551.2016.1214557>
- He X, Tan C, Wang F, Wang Y, Zhou R, Cui D, You W, Zhao H, Ren J, Feng B (2016) Knock-in of large reporter genes in human cells via CRISPR/Cas9-induced homology-dependent and independent DNA repair. *Nucleic Acids Res* 44(9):e85. <https://doi.org/10.1093/nar/gkw064>
- Hiller GW, Ovalle AM, Gagnon MP, Curran ML, Wang WG (2017) Cell-controlled hybrid perfusion fed-batch CHO cell process provides significant productivity improvement over conventional fed-batch cultures. *Biotechnol Bioeng* 114(7):1438–1447. <https://doi.org/10.1002/bit.26259>
- Inniss MC, Bandara K, Jusiak B, Lu TK, Weiss R, Wroblewska L, Zhang L (2017) A novel Bxb1 integrase RMCE system for high fidelity site-specific integration of mAb expression cassette in CHO cells. *Biotechnol Bioeng* 114(8):1837–1846. <https://doi.org/10.1002/bit.26268>
- Irion U, Krauss J, Nusslein-Volhard C (2014) Precise and efficient genome editing in zebrafish using the CRISPR/Cas9 system. *Development* 141(24):4827–4830. <https://doi.org/10.1242/dev.115584>
- Jabalameli HR, Zahednasab H, Karimi-Moghaddam A, Jabalameli MR (2015) Zinc finger nuclease technology: advances and obstacles in modelling and treating genetic disorders. *Gene* 558(1):1–5. <https://doi.org/10.1016/j.gene.2014.12.044>
- Josse L, Xie J, Proud CG, Snales CM (2016) mTORC1 signalling and eIF4E/4E-BP1 translation initiation factor stoichiometry influence recombinant protein productivity from GS-CHOK1 cells. *Biochem J* 473(24):4651–4664. <https://doi.org/10.1042/BJC20160845>
- Kawabe Y, Shimomura T, Huang S, Imanishi S, Ito A, Kamihira M (2016) Targeted transgene insertion into the CHO cell genome using Cre recombinase-incorporating integrase-defective retroviral vectors. *Biotechnol Bioeng* 113(7):1600–1610. <https://doi.org/10.1002/bit.25923>
- Kawabe Y, Komatsu S, Komatsu S, Murakami M, Ito A, Sakuma T, Nakamura T, Yamamoto T, Kamihira M (2017) Targeted knock-in of an scFv-Fc antibody gene into the hprt locus of Chinese hamster ovary cells using CRISPR/Cas9 and CRIS-PITCh systems. *J Biosci Bioeng*. <https://doi.org/10.1016/j.jbiosc.2017.12.003>
- Kleinstiver BP, Pattanayak V, Prew MS, Tsai SQ, Nguyen NT, Zheng Z, Joung JK (2016) High-fidelity CRISPR-Cas9 nucleases with no detectable genome-wide off-target effects. *Nature* 529(7587):490–495. <https://doi.org/10.1038/nature16526>
- Lai T, Yang Y, Ng SK (2013) Advances in mammalian cell line development technologies for recombinant protein production. *Pharmaceuticals (Basel)* 6(5):579–603. <https://doi.org/10.3390/ph6050579>
- Lee JS, Kallehauge TB, Pedersen LE, Kildegaard HF (2015) Site-specific integration in CHO cells mediated by CRISPR/Cas9 and homology-directed DNA repair pathway. *Sci Rep* 5:8572. <https://doi.org/10.1038/srep08572>
- Lee JS, Grav LM, Pedersen LE, Lee GM, Kildegaard HF (2016) Accelerated homology-directed targeted integration of transgenes in Chinese hamster ovary cells via CRISPR/Cas9 and fluorescent enrichment. *Biotechnol Bioeng* 113(11):2518–2523. <https://doi.org/10.1002/bit.26002>
- Li S, Gao X, Peng R, Zhang S, Fu W, Zou F (2016) FISH-based analysis of clonally derived CHO cell populations reveals high probability for transgene integration in a terminal region of chromosome 1 (1q13). *PLoS One* 11(9):e0163893. <https://doi.org/10.1371/journal.pone.0163893>
- Mali P, Aach J, Stranges PB, Esvelt KM, Moosburner M, Kosuri S, Yang L, Church GM (2013) CAS9 transcriptional activators for target specificity screening and paired nickases for cooperative genome engineering. *Nat Biotechnol* 31(9):833–838. <https://doi.org/10.1038/nbt.2675>
- Moreno-Mateos MA, Vejnár CE, Beaudoin JD, Fernandez JP, Mis EK, Khokha MK, Giraldez AJ (2015) CRISPRscan: designing highly efficient sgRNAs for CRISPR-Cas9 targeting in vivo. *Nat Methods* 12(10):982–988. <https://doi.org/10.1038/nmeth.3543>
- Nakao H, Harada T, Nakao K, Kiyonari H, Inoue K, Furuta Y, Aiba A (2016) A possible aid in targeted insertion of large DNA elements by CRISPR/Cas in mouse zygotes. *Genesis* 54(2):65–77. <https://doi.org/10.1002/dvg.22914>
- Ran FA, Hsu PD, Lin CY, Gootenberg JS, Konermann S, Trevino AE, Scott DA, Inoue A, Matoba S, Zhang Y, Zhang F (2013) Double nicking by RNA-guided CRISPR Cas9 for enhanced genome editing specificity. *Cell* 154(6):1380–1389. <https://doi.org/10.1016/j.cell.2013.08.021>
- Ritter A, Rauschert T, Oertli M, Piehlmaier D, Mantas P, Kuntzelmann G, Lageyre N, Brannetti B, Voedisch B, Geisse S, Jostock T, Laux H (2016) Disruption of the gene C12orf35 leads to increased productivities in recombinant CHO cell lines. *Biotechnol Bioeng* 113(11):2433–2442. <https://doi.org/10.1002/bit.26009>
- Sakuma T, Takenaga M, Kawabe Y, Nakamura T, Kamihira M, Yamamoto T (2015) Homologous recombination-independent large gene cassette knock-in in CHO cells using TALEN and MMEJ-directed donor plasmids. *Int J Mol Sci* 16(10):23849–23866. <https://doi.org/10.3390/ijms161023849>
- Sun T, Li CD, Han L, Jiang H, Xie YQ, Zhang BH, Qian XP, Lu HL, Zhu JW (2015) Functional knockout of FUT8 in Chinese hamster ovary cells using CRISPR/Cas9 to produce a defucosylated antibody. *Eng Life Sci* 15(6):660–666. <https://doi.org/10.1002/elsc.201400218>
- Templeton N, Lewis A, Dorai H, Qian EA, Campbell MP, Smith KD, Lang SE, Betenbaugh MJ, Young JD (2014) The impact of anti-apoptotic gene Bcl-2 expression on CHO central metabolism. *Metab Eng* 25: 92–102. <https://doi.org/10.1016/j.ymben.2014.06.010>
- Wang C, Thudium KB, Han M, Wang XT, Huang H, Feingersh D, Garcia C, Wu Y, Kuhne M, Srinivasan M, Singh S, Wong S, Garner N, Leblanc H, Bunch RT, Blanset D, Selby MJ, Korman AJ (2014) In vitro characterization of the anti-PD-1 antibody nivolumab, BMS-936558, and in vivo toxicology in non-human primates. *Cancer Immunol Res* 2(9):846–856. <https://doi.org/10.1158/2326-6066.CIR-14-0040>
- Wang X, Kawabe Y, Kato R, Hada T, Ito A, Yamana Y, Kondo M, Kamihira M (2017) Accumulative scFv-Fc antibody gene integration into the hprt chromosomal locus of Chinese hamster ovary cells. *J Biosci Bioeng* 124(5):583–590. <https://doi.org/10.1016/j.jbiosc.2017.05.017>
- Xu S, Chen H (2016) High-density mammalian cell cultures in stirred-tank bioreactor without external pH control. *J Biotechnol* 231:149–159. <https://doi.org/10.1016/j.jbiotec.2016.06.019>
- Zhu J (2012) Mammalian cell protein expression for biopharmaceutical production. *Biotechnol Adv* 30(5):1158–1170. <https://doi.org/10.1016/j.biotechadv.2011.08.022>
- Zhu J (2013) Update on production of recombinant therapeutic protein: transient gene expression. *Smithers Rapra Technology Ltd*.
- Zong H, Han L, Ding K, Wang J, Sun T, Zhang X, Cagliero C, Jiang H, Xie Y, Xu J, Zhang B, Zhu J (2017) Producing defucosylated antibodies with enhanced in vitro antibody-dependent cellular cytotoxicity via FUT8 knockout CHO-S cells. *Eng Life Sci* 17(7):801–808. <https://doi.org/10.1002/elsc.201600255>